DOI:10.1021/ic9003356

Inorganic Chemistry
Article

Reversible Water Intercalation Accompanied by Coordination and Color Changes in a Layered Metal−Organic Framework

Partha Mahata, K. V. Ramya, and Srinivasan Natarajan*

Framework Solids Laboratory, Solid State and Structural Chemistry Unit, Indian Institute of Science, Bangalore 560 012, India

Received February 19, 2009

A new two-dimensional 3d−4f mixed-metal mixed dicarboxylate (homocyclic and heterocyclic) of the formula $[Gd_2(H_2O)_2Ni(H_2O)_2(1,2\text{-bdc})_2(2,5\text{-pydc})_2]\cdot 8H_2O$ (**1**; 1,2-H_2bdc = 1,2-benzenedicarboxylic acid and 2,5-H_2pydc = 2,5-pyridinedicarboxylic acid) has been prepared by employing the hydrothermal method. The structure has infinite one-dimensional −Gd−O−Gd− chains formed by the edge-shared GdO_9 polyhedral units, resulting exclusively from the connectivity between the Gd^{3+} ions and the 1,2-bdc units. The chains are connected by the $[Ni(H_2O)_2(2,5\text{-pydc})_2]^{2-}$ metalloligand, forming the two-dimensional layer arrangements. The stacking of the layers creates hydrophilic and hydrophobic spaces in the interlamellar region. A one-dimensional water ladder structure, formed by the extraframework water molecules, occupies the hydrophilic region while the benzene ring of 1,2-bdc occupies the hydrophobic region. To the best of our knowledge, the present compound represents the first example of a 3d−4f mixed-metal carboxylate in which two different aromatic dicarboxylate anions act as the linkers. The stabilization energies of the water clusters have been evaluated using density functional theory calculations. The water molecules in **1** are fully reversible accompanied by a change in color (greenish blue to brown) and coordination around Ni^{2+} ions (octahedral to distorted tetrahedral).

Introduction

The research in the area of metal−organic frameworks (MOFs) continues to be interesting for their unique structures and tunable properties.[1] Many of the known MOFs have three-dimensional structures, and the synthesis of two-dimensional ones is also important because some of them can replicate the behavior of naturally occurring clays.[2] The layered compounds can also participate in a variety of host−guest chemistries such as photopolymerization reactions, catalysis, etc.[3] The guest molecules can play a useful role in the control of crystal structures and the physical and chemical behavior of two-dimensional host lattices.[4]

Though the formation of layered MOFs based on single-metal ions has been established, reports on the use of two different metal ions are few.[5] We have been interested in the

*Corresponding author. E-mail: snatarajan@sscu.iisc.ernet.in.

(1) (a) Morris, R. E.; Wheatley, P. S. *Angew. Chem., Int. Ed.* **2008**, *47*, 4966. (b) Furukawa, H.; Kim, J.; Ockwig, N. W.; O'Keeffe, M.; Yaghi, O. M. *J. Am. Chem. Soc.* **2008**, *130*, 11650. (c) Horike, S.; Dinca, M.; Tamaki, K.; Long, J. R. *J. Am. Chem. Soc.* **2008**, *130*, 5854. (d) Maspoch, D.; Ruiz-Molina, D.; Veciana, J. *Chem. Soc. Rev.* **2007**, *36*, 770. (e) Goto, Y.; Sato, H.; Shinkai, S.; Sada, K. *J. Am. Chem. Soc.* **2008**, *130*, 14354. (f) Rao, C. N. R.; Natarajan, S.; Vaidhanathan, R. *Angew. Chem., Int. Ed.* **2004**, *43*, 1466. (g) Eddaoudi, M.; Kim, J.; Vodak, D.; Sudik, A.; Wachter, J.; O'Keefe, M.; Yaghi, O. M. *Proc. Natl. Acad. Sci. U.S.A.* **2002**, *99*, 4900. (h) Kitawaga, S.; Kitaura, R.; Noro, S. *Angew. Chem., Int. Ed.* **2004**, *43*, 2334. (i) Bradshaw, D.; Warren, J. E.; Rosseinsky, M. J. *Science* **2007**, *315*, 977. (j) Ferey, G.; Draznieks, C. M.; Serre, C.; Millange, F.; Dutour, J.; Surble, S.; Margiolaki, I. *Science* **2005**, *309*, 2040. (k) Maji, T. K.; Matsuda, R.; Kitwaga, S. *Nat. Mater.* **2007**, *6*, 142.

(2) Chen, C. L.; Beatty, A. M. *J. Am. Chem. Soc.* **2008**, *130*, 17222.

(3) (a) Matsumoto, A.; Sada, K.; Tashiro, K.; Miyata, M.; Tsubouchi, T.; Tanaka, T.; Odani, T.; Nagahama, S.; Tanaka, T.; Inoue, K.; Saragai, S.; Nakamoto, S. *Angew. Chem., Int. Ed.* **2002**, *41*, 2502. (b) Nakano, K.; Sada, K.; Nakagawa, K.; Aburaya, K.; Yoswathananont, N.; Tohnai, N.; Miyata, M. *Chem.—Eur. J.* **2005**, *11*, 1725. (c) Reddy, D. S.; Duncan, S.; Shimizu, G. K. H. *Angew. Chem., Int. Ed.* **2003**, *42*, 1360.

(4) (a) Tanaka, D.; Kitagawa, S. *Chem. Mater.* **2008**, *20*, 922. (b) Holman, K. T.; Pivovar, A. M.; Swift, J. A.; Ward, M. D. *Acc. Chem. Res.* **2001**, *34*, 107. (c) Holman, K. T.; Pivovar, A. M.; Ward, M. D. *Science* **2001**, *294*, 1907. (d) Beatty, A. M.; Granger, K. E.; Simpson, A. E. *Chem.—Eur. J.* **2002**, *8*, 3254. (e) Beatty, A. M.; Schneider, C. M.; Simpson, A. E.; Zaher, J. L. *CrystEngComm* **2002**, *4*, 282. (f) Biradha, K.; Dennis, D.; MacKinnon, V. A.; Sharma, C. V. K.; Zaworotko, M. J. *J. Am. Chem. Soc.* **1998**, *120*, 11894. (g) Yuge, T.; Miyata, M.; Tohnai, N. *Cryst. Growth Des.* **2006**, *6*, 1271. (h) Sada, K.; Inoue, K.; Tanaka, T.; Epergyes, A.; Tanaka, A.; Tohnai, N.; Matsumoto, A.; Miyata, M. *Angew. Chem., Int. Ed.* **2005**, *44*, 7059. (i) Oshita, S.; Matsumoto, A. *Chem.—Eur. J.* **2006**, *12*, 2139. (j) Mallouk, T. E.; Gavin, J. A. *Acc. Chem. Res.* **1998**, *31*, 209.kMitzi, D. B. In *Functional Hybrid Materials*; Gomez-Romero, P., Sanchez, C., Eds.; Wiley-VCH Verlag GmbH & Co. KGaA: Weinheim, Germany, 2004. (l) Song, J. L.; Mao, J. G.; Sun, Y. Q.; Zeng, H. Y.; Kremer, R. K.; Clearfield, A. J. Solid State Chem. 2004, 177, 633.

(5) (a) Wang, F. Q.; Zheng, X. J.; Wan, Y. H.; Sun, C. Y.; Wang, Z. M.; Wang, K. Z.; Jin, L. P. *Inorg. Chem.* **2007**, *46*, 2956. (b) Kim, Y. J.; Park, Y. J.; Jung, D. Y. *Dalton Trans.* **2005**, 2603. (c) He, F.; Tong, M. L.; Yu, X. L.; Chen, X. M. *Inorg. Chem.* **2005**, *44*, 559. (d) Zhang, J. J.; Xia, S. Q.; Sheng, T. L.; Hu, S. M.; Leibeling, G.; Meyer, F.; Wu, X. T.; Xiang, S. C.; Fu, R. B. *Chem. Commun.* **2004**, 1186. (e) Yu, Z. T.; Liao, Z. L.; Jiang, Y. S.; Li, G. H.; Chen, J. S. *Chem.—Eur. J.* **2005**, *11*, 2642.

Published on Web 4/17/2009

study of the formation of MOFs using both transition metals and lanthanides, which resulted in a layered solid, $[Gd(H_2O)_3Co\{C_5N_1H_3(COO)_2\}_3]$.[6] Our continued investigations also revealed the formation of a new pillared layered structure by use of two different carboxylic acids (homocyclic and heterocyclic), $[La_2(H_2O)_4][\{C_5H_3N(COO)_2\}_2\{C_6H_4(COO)_2\}]$.[7] Similarly, we wanted to investigate whether it would be possible to prepare a 3d−4f mixed-metal mixed-dicarboxylate (benzene and pyridine) compound. During the course of these studies, we have now prepared a new 3d−4f mixed-metal compound formed with benzene-1,2-dicarboxylate and pyridine-2,5-dicarboxylate, $[Gd_2(H_2O)Ni(H_2O)_2(1,2\text{-bdc})_2(2,5\text{-pydc})_2].8H_2O$ (**1**). The structure contains cationic one-dimensional gadolinium phthalate chains, $[Gd(1,2\text{-bdc})]^+$, connected by an anionic $[Ni(H_2O)_2(2,5\text{-pydc})_2]^{2-}$ metalloligand, forming a two-dimensional structure with decorated Kagome topology. The structure contains one-dimensional water ladders in the interlamellar space, which can be reversibly adsorbed. The removal of water is also accompanied by a change in color from light greenish blue to brown. In this paper, we present the synthesis, structure, reversible adsorption, and also stability studies of the water assembly of **1**.

Experimental Section

Synthesis and Initial Characterization. The title compound was prepared by employing the hydrothermal method. Gd_2O_3 (0.09 g, 0.25 mM) and $Ni(OAc)_2\cdot 4H_2O$ (0.127 g, 0.5 mM) were dispersed in 7 mL of water. 2,5-Pyridinedicarboxylic acid (0.1705 g, 1 mM), 1,2-benzenedicarboxylic acid (0.1678 g, 1 mM), and NaOH (0.08 g, 2 mM) were added with continuous stirring, and the mixture was homogenized at room temperature for 30 min. The final reaction mixture was sealed in a 23 mL poly(tetrafluoroethylene)-lined stainless steel autoclave and heated at 180 °C for 72 h. The initial pH value of the reaction mixture was 3, and no appreciable change in the pH was noted after the reaction. The final product, containing large quantities of light-greenish-blue rectangular crystals, was filtered, washed with deionized water under vacuum, and dried at ambient conditions (yield 70% based on Gd). Elem anal. Calcd for **1**: C, 28.85; H, 3.05; N, 2.24. Found: C, 28.62; H, 3.11; N, 2.31. Energy-dispersive analysis of X-ray analysis on many single crystals revealed a Gd/Ni ratio of 2:1.

Powder X-ray diffraction (PXRD) patterns were recorded on well-ground samples in the 2θ range of 5−50° using Cu Kα radiation (Philips X'pert; see the Supporting Information, Figure S1). The X-ray diffraction (XRD) patterns indicated that the product is a new material, with the pattern being entirely consistent with the simulated XRD pattern generated based on the structure determined using the single-crystal XRD. The IR spectrum was recorded on a KBr pellet (Perkin-Elmer, SPECTRUM 1000; see Supporting Information, Figure S2). The observed IR frequencies are listed in Table 1.

Single-Crystal Structure Determination. A suitable single crystal was carefully selected under a polarizing microscope and carefully glued to a thin glass fiber. The single-crystal data were collected on a Bruker AXS SMART Apex CCD diffractometer at 293(2) K. The X-ray generator was operated at 50 kV and 35 mA using Mo Kα (λ = 0.710 73 Å) radiation. Data were collected with an ω scan width of 0.3°. A total of 606 frames were collected in three different settings of φ (0, 90, and 180°), keeping the sample-to-detector distance fixed at 6.03 cm and the detector position (2θ) fixed at −25°. The data were reduced using *SAINTPLUS*,[8] and an empirical absorption correction was applied using the *SADABS* program.[9] The structure was solved and refined using *SHELXL97*[10] present in the *WinGx* suite of programs (version 1.63.04a).[11] All of the hydrogen atoms of the carboxylic acids and the water molecules were initially located in the difference Fourier maps, and for the final refinement, the hydrogen atoms were placed in geometrically ideal positions and held in the riding mode. Final refinement included atomic positions for all of the atoms, anisotropic thermal parameters for all of the non-hydrogen atoms, and isotropic thermal parameters for all of the hydrogen atoms. Full-matrix least-squares refinement against $|F^2|$ was carried out using the *WinGx* package of programs.[11] Details of the structure solution and final refinements are given in Table 2. CCDC 650346 contains the crystallographic data for this paper. These data can be obtained free of charge from the Cambridge Crystallographic Data Center (CCDC) via www.ccdc.cam.ac.uk/data_request/cif.

Results and Discussion

Structure. The compound has 32 non-hydrogen atoms in the asymmetric unit, of which one Gd^{3+} ion and one Ni^{2+} ion are crystallography independent. Of these, the Ni^{2+} ions occupy a special position (2b) with a site occupancy of 0.5. There are one 1,2-bdc anion and one 2,5-pydc anion present in the asymmetric unit (see the Supporting Information, Figure S3). The two carboxylate groups of 1,2-bdc are connected only with the Gd^{3+} ions. Two of the carboxylate oxygen atoms [O(1) and O(5)] of 1,2-bdc have μ_3 connectivity (connects two Gd^{3+} ions and a carbon atom). The two carboxylate groups of 2,5-pydc show differences in connectivity: the carboxylate group at the 2 position of the pyridine ring has simple monodentate connectivity with the Ni^{2+} ion, whereas the carboxylate group at the 5 position of the pyridine ring has bidentate connectivity with two Gd^{3+} ions. The nitrogen atom of the pyridine ring is bonded with the Ni^{2+} ion (see the Supporting Information, Figure S4).

The Gd^{3+} ion is coordinated by nine oxygen atoms and has a distorted tricapped trigonal-prismatic environment [GdO_9, CN = 9]. Of the nine oxygen atoms, one oxygen atom, [O(6)], is a coordinated water molecule and the remaining ones are from the carboxylate group (1,2-bdc and 2,5-pydc). The Ni^{2+} ion is coordinated by four oxygen atoms and two nitrogen atoms from the pyridine ring, forming a distorted octahedral environment [NiO_4N_2, CN = 6]. Of the four oxygen atoms, two symmetry-generated oxygen atoms [O(11)] are coordinated water molecules and the remaining two oxygen atoms are from the carboxylate group (2,5-pydc). The Gd−O bonds have an average distance of 2.45 Å, and the Ni−O and Ni−N bonds have average distances of 2.08 and 2.05 Å, respectively. The O−Gd−O bond angles are in the range of 50.71(7)−167.03(7)°, and the

(6) Mahata, P.; Sankar, G.; Madras, G.; Natarajan, S. *Chem. Commun.* **2005**, 5787.

(7) Mahata, P.; Ramya, K. V.; Natarajan, S. *Chem.—Eur. J.* **2008**, *14*, 5839.

(8) *SMART* (version 5.628), *SAINT* (version 6.45a), *XPREP*, and *SHELXTL*; Bruker AXS Inc.: Madison, WI, 2004.

(9) Sheldrick, G. M. *Siemens area correction absorption correction program*; University of Göttingen: Göttingen, Germany, 1994.

(10) Sheldrick, G. M. *SHELXL-97 program for crystal structure solution and refinement*; University of Göttingen: Göttingen, Germany, 1997.

(11) Farrugia, J. L., WinGx suite for small-molecule single crystal crystallography. *J. Appl. Crystallogr.*, 1999, 32, 837.

Table 1. Observed IR Bands for **1**

bands	ν(H$_2$O)	δ(H$_2$O)	ν_{as}(COO) [single coordination]	ν_{as}(COO) [double coordination]	ν_{as}(COO) [triple coordination]	N$_s$(COO) [triple coordination]	ν_a(COO) [doublec oordination]	ν_a(COO) [single coordination]	δ(CH$_{aromatic}$) in-plane	δ(CH$_{aromatic}$) out-of-plane	δ(COO)
wavenumber (cm^{-1})	3000−3600(s)	1620(s)	1592(s)	1554(s)	1542(s)	1415(s)	1392(s)	1366(s)	1130−1040(m)	880−810(m)	760−650(m)

Table 2. Crystal Data and Structure Refinement Parameters for **1**[a]

empirical formula	$C_{30}H_{38}N_2O_{28}Gd_2Ni$
fw	1247.84
cryst syst	monoclinic
space group	$P2_1/c$ (No. 14)
a (Å)	12.791(2)
b (Å)	7.2645(13)
c (Å)	23.439(4)
α (deg)	90.0
β (deg)	98.450(3)
γ (deg)	90.0
V (Å^3)	2154.3(7)
Z	2
T (K)	293(2)
ρ_{calc} (g cm^{-3})	1.924
μ (mm^{-1})	3.573
θ range (deg)	2.20−28.01
λ(Mo Kα) (Å)	0.710 73
R indices [$I > 2\sigma(I)$]	R1 = 0.0278, wR2 = 0.0504
R indices (all data)	R1 = 0.0368, wR2 = 0.0530

[a] $R1 = \sum||F_o| - |F_c||/\sum|F_o|$; $wR2 = \{\sum[w(F_o^2 - F_c^2)^2]/\sum[w(F_o^2)^2]\}^{1/2}$. $w = 1/[\sigma^2(F_o)^2 + (aP)^2 + bP]$, $P = [\max(F_o^2, 0) + 2(F_c)^2]/3$, where $a = 0.0184$ and $b = 0.8239$.

Table 3. Selected Bond Distances (Å) Observed in **1**

bond	amplitude	bond	amplitude
Gd(1)−O(1)	2.526(2)	Gd(1)−O(7)	2.349(2)
Gd(1)−O(2)	2.601(2)	Gd(1)−O(1)#1[a]	2.382(2)
Gd(1)−O(3)	2.358(2)	Gd(1)−O(5)#2[a]	2.429(2)
Gd(1)−O(4)	2.459(2)	Ni(1)−O(11)	2.121(3)
Gd(1)−O(5)	2.5789(19)	Ni(1)−O(12)	2.042(2)
Gd(1)−O(6)	2.359(2)	Ni(1)−N(1)	2.051(2)

[a] Symmetry transformations used to generate equivalent atoms: #1, $-x, y - {}^1/_2, -z + {}^1/_2$; #2, $-x, y + {}^1/_2, -z + {}^1/_2$.

O/N−Ni−O/N bond angles are in the range of 80.17 (9)−180.0(9)°. The selected bond distances are listed in Table 3.

The two-dimensional structure of the compound can be simplified by considering the connectivity between the GdO$_9$ polyhedra. Thus, each of the GdO$_9$ polyhedral units are connected via the μ_3 carboxylate oxygen atoms [O(1) and O(5)] by sharing the edges to give rise to infinite −Gd−O−Gd− chains, with a Gd−Gd distance of 3.991 Å (see the Supporting Information, Figure S5). The cationic −Gd−O−Gd− chains are formed exclusively by the 1,2-bdc units (Figure 1a). The Ni^{2+} ions are connected by two 2,5-pydc anions and two water molecules, forming a typical dianionic, $[Ni(H_2O)_2(pydc)_2]^{2-}$, metalloligand (Figure 1b). The metalloligand connects the gadolinium carboxylate chains, giving rise to a neutral two-dimensional structure (Figure 1c). The layers are arranged in such a way that there are exclusive regions in the interlamellar region that are hydrophilic and hydrophobic (Figure 2a). The hydrophilic regions are due to the presence of guest water molecules, coordinated water molecules [O(6) and O(11)], and carboxylate oxygen atoms (see the Supporting Information, Figure S6). The projecting aromatic phthalate units form the hydrophobic regions.

Layer formation is essentially facilitated by the connectivity between Ni^{2+} and 2,5-pydc, which also connects the gadolinium phthalate chains. The phthalate units do not contribute to the formation of the network connectivity except providing the necessary oxygen atoms needed for the nine-coordinated Gd^{3+} ions. To analyze the topology of the layer, we can consider the connectivity of 2,5-pydc with the Gd^{3+} and Ni^{2+} ions. Here, each Ni^{2+} ion is connected with four Gd^{3+} ions and each

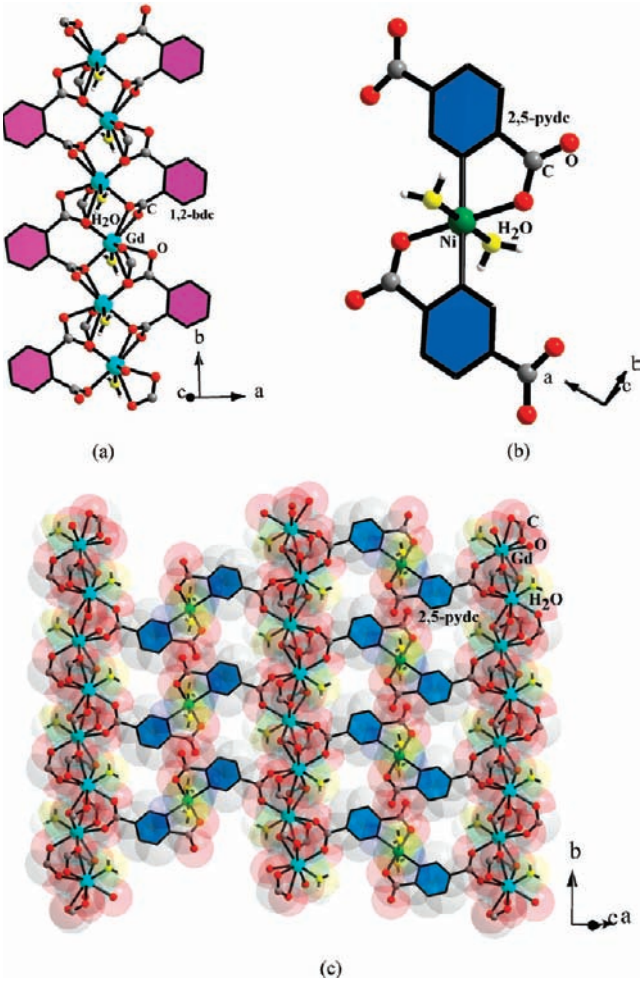

Figure 1. (a) One-dimensional −Gd−O−Gd− chains formed by the connectivity between 1,2-bdc and the Gd^{3+} ions in **1**. (c) Structure of the dianionic, $[Ni(H_2O)_2(pydc)_2]^{2-}$, metalloligand. (d) Layered structure formed from the connectivity between the $[Ni(H_2O)_2(pydc)_2]^{2-}$ metalloligand and the −Gd−O−Gd− chains. The 1,2-bdc unit has been shown partially for clarity.

Gd^{3+} ion is connected with two Ni^{2+} ions and two Gd^{3+} ions through the 2,5-pydc ligands (Figure 1c). Thus, both of the Gd^{3+} and Ni^{2+} ions act as the four-connected node, and the connectivity between them gives

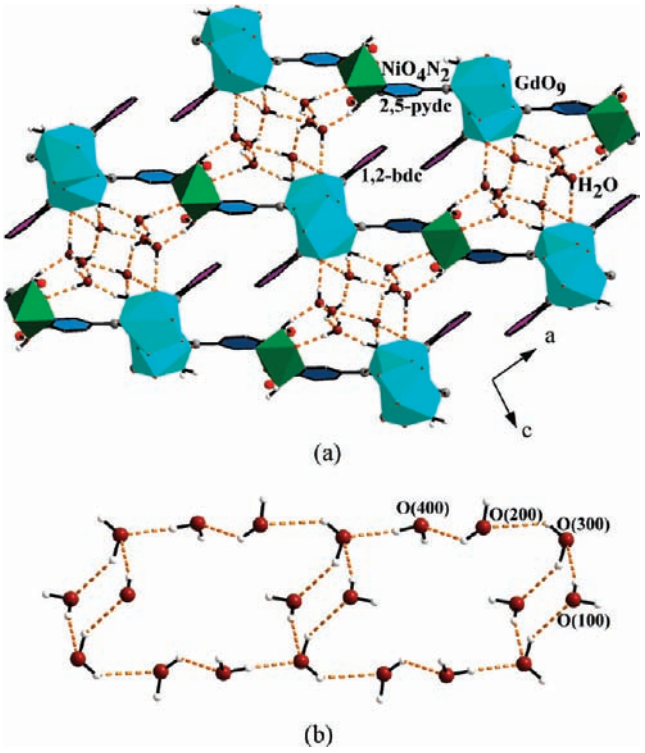

Figure 2. (a) Arrangement of the layers in **1**. Note the presence of alternate hydrophobic and hydrophilic regions. (b) View of the arrangement of the one-dimensional water cluster units (ladder) in **1**.

rise to a network with two triangles and two hexagons around the node (see the Supporting Information, Figure S7), which is similar to that found in two-dimensional Kagome networks.

A careful analysis of the structure reveals that the extraframework water molecules [O(100), O(200), O (300), and O(400)] form cooperative hydrogen-bond interactions, giving rise to a ladderlike one-dimensional structure (Figure 2b). Thus, the water molecules O(100) and O(300) form a tetrameric unit because of the presence of a center of symmetry, while the water molecules O(200) and O(400) form a simple dimer. The connectivity between the two units forms the one-dimensional water ladder (Figure 2b). The one-dimensional water ladder also forms extensive hydrogen-bond interactions with the coordinated water molecules [O(6) and O(11)] (see the Supporting Information, Figure S8), giving rise to a new type of water assembly in this structure. Further analysis of the water cluster also reveals some interesting aspects. Thus, all of the extraframework water molecules, O(100), O(200), O(300), and O(400), have a tetrahedral arrangement with other water molecules and the carboxylate oxygen atoms (see the Supporting Information, Figure S9). This is similar to the arrangement of the water molecules in ice with active participation from the lone pair of the oxygen atoms. The coordinated water molecules, O(6) and O(11), however, have a trigonal arrangement with regards to other water molecules and the carboxylate oxygen atoms. All of the water molecules, however, appear to position themselves in such a way as to form a distorted α-Po-like topology (see the Supporting Information, Figure S10).

(12) Buck, U.; Huisken, F. *Chem. Rev.* **2000**, *100*, 3863.

Water is important for the study of many of biological processes.[12] The identification of water clusters in diverse environments can lead to a better understanding of the behavior of the water molecule. Up to now, water clusters, $(H_2O)_n$, with $n = 2-8, 10, 12, 14, 16, 18$, and 45, have been obtained in diverse hosts.[13−23] Among all of the water clusters, the one-dimensional water structure appears to draw considerable interest because of its importance in biology.[24] One-dimensional water structures are generally built from an infinite connection of water molecules[25] or through the linking of one or more types of smaller cyclic water clusters.[26] In light of this, formation of the water ladder in the present system by connectivity of the tetramer and dimer units is new.

Stability Studies of the Water Cluster. The observation of the water ladders in the present structure prompted us to investigate the stability of such water clusters using simple theoretical models. We have also performed studies on similar one-dimensional water clusters that have been observed in other related systems of compounds in the literature (Table 4). To understand the stability of the one-dimensional water ladder in **1**, we have carried out an ab initio calculation using density functional theory. To aid in our understanding, we have also calculated the stabilization energies of water clusters having one-dimensional connectivity similar to that found in other MOFs

(13) For $(H_2O)_2$: Manikumari, S.; Shivaiah, V.; Das, S. K. *Inorg. Chem.* **2002**, *41*, 6953.
(14) For $(H_2O)_3$: (a) Macgillivary, L. R.; Atwood, J. L. *J. Am. Chem. Soc.* **1997**, *199*, 22592. (b) Keutsch, F. N.; Cruzan, J. D.; Saykally, R. J. *Chem. Rev.* **2003**, *103*, 2533.
(15) For $(H_2O)_4$: (a) Supriya, S.; Manikumari, S.; Raghavaiah, P.; Das, S. K. *New J. Chem.* **2003**, *27*, 218. (b) Supriya, S.; Das, S. K. *New J. Chem.* **2003**, *27*, 1568. (c) Long, L. S.; Wu, Y. S.; Huang, R. B.; Zheng, L. S. *Inorg. Chem.* **2004**, *43*, 3798. (d) Tao, J.; Ma, Z. J.; Huang, R. B.; Zheng, L. S. *Inorg. Chem.* **2004**, *43*, 6133. (e) Sun, Y. Q.; Zhang, J.; Ju, Z. F.; Yang, G. Y. *Aust. J. Chem.* **2005**, *58*, 572. (f) Mahata, P.; Natarajan, S. *Inorg. Chem.* **2007**, *46*, 1250.
(16) For $(H_2O)_6$: (a) Moorthy, J. N.; Natarajan, R.; Venugopalan, P. *Angew. Chem., Int. Ed.* **2002**, *41*, 3417. (b) Ghosh, S. K.; Bharadwaj, P. K. *Inorg. Chem.* **2003**, *42*, 8250. (c) Ghosh, S. K.; Bharadwaj, P. K. *Inorg. Chem.* **2004**, *43*, 5180. (d) Ye, B. H.; Ding, B. B.; Weng, Y. Q.; Chen, X. M. *Inorg. Chem.* **2004**, *43*, 6866. (e) Liao, Y. C.; Jiang, Y. C.; Wang, S. L. *J. Am. Chem. Soc.* **2005**, *127*, 12794.
(17) For $(H_2O)_8$: (a) Atwoood, J. L.; Barbour, L. J.; Ness, T. J.; Raston, C. L.; Raston, P. L. *J. Am. Chem. Soc.* **2001**, *123*, 7192. (b) Doedens, R. J.; Yohannes, E.; Kahn, M. I. *Chem. Commun.* **2002**, 62. (c) Ma, B. Q.; Sun, H. L.; Gao, S. *Chem. Commun.* **2005**, 2336. (d) Prasad, T. K.; Rajasekharan, M. V. *Cryst. Growth Des.* **2006**, *6*, 488. (e) Ghosh, S. K.; Bharadwaj, P. K. *Eur. J. Inorg. Chem.* **2005**, *24*, 4886.
(18) For $(H_2O)_{10}$: (a) Barbour, L. J.; Orr, G. W.; Atwood, J. L. *Nature (London)* **1998**, *393*, 671. (b) Barbour, L. J.; Orr, G. W.; Atwood, J. L. *Chem. Commun.* **2000**, 859. (c) Michaelides, A.; Skoulika, S.; Bakalbassis, E. G.; Mrozinski, J. *Cryst. Growth Des.* **2003**, *3*, 487. (d) Bergougant, R. D.; Robin, A. Y.; Fromm, K. M. *Cryst. Growth Des.* **2005**, *5*, 1691.
(19) For $(H_2O)_{12}$: (a) Ghosh, S. K.; Bharadwaj, P. K. *Angew. Chem., Int. Ed.* **2004**, *43*, 3577. (b) Neogi, S.; Savitha, G.; Bharadwaj, P. K. *Inorg. Chem.* **2004**, *43*, 3771.
(20) For $(H_2O)_{14}$: Ghosh, S. K.; Ribas, J.; Fallah, M. S. E.; Bharadwaj, P. K. *Inorg. Chem.* **2005**, *44*, 3856.
(21) For $(H_2O)_{16}$: Ghosh, S. K.; Bharadwaj, P. K. *Inorg. Chem.* **2004**, *43*, 6887.
(22) For $(H_2O)_{18}$: Raghuraman, K.; Katti, K. K.; Barbour, L. J.; Pillarsetty, N.; Barnes, C. L.; Katti, K. V. *J. Am. Chem. Soc.* **2003**, *125*, 6955.
(23) For $(H_2O)_{45}$: Lakshminarayanan, P. S.; Suresh, E. I.; Ghosh, P. *J. Am. Chem. Soc.* **2005**, *127*, 13132.
(24) (a) Sainz, G.; Carrell, C. J.; Ponamerev, M. V.; Soriano, G. M.; Cramer, W. A.; Smith, J. L. *Biochemistry* **2000**, *39*, 9164. (b) Jude, K. M.; Wright, S. K.; Tu, C.; Silverman, D. N.; Viola, R. E.; Christianson, D. W. *Biochemistry* **2002**, *41*, 2485. (c) Tajkhorshid, K.; Nollert, P.; Jensen, M. Ø.; Miercke, L. J. W.; O'Connell, J.; Stroud, R. M.; Schulten, K. *Science* **2002**, *296*, 525.

Table 4. One-Dimensional Water Structures Observed in Other Host−Guest Systems

serial no.	formula	smallest water cluster, $(H_2O)_n$	total size of repeating unit, $(H_2O)_n$	ref
1	$[Gd_2(H_2O)_2Ni(H_2O)_2(1,2\text{-bdc})_2(2,5\text{-pydc})_2]\cdot 8H_2O$ (1,2-H_2bdc = 1,2-benzenedicarboxylic acid; 2,5-H_2pydc = 2,5-pyridinedicarboxylic acid)	n = 2, 4	n = 12	present compound
2	$[TACD]\cdot 3H_2O$ (TACD = 1,4,7,10-tetraazacyclododecane)	n = 4	n = 10	26a
3	[Cd(phen)(Hpppn)].$4H_2O$ (phen = 1,10-phenanthroline; pppn = 3-phosphonopropionate)	n = 6	n = 14	26b
4	$[Cu^{I}_2Cu^{II}(pydc)_2(bpe)_2]\cdot 7H_2O$ (pydc = pyridine-2,6-dicarboxylate; bpe = *trans*-1,2-bis(4-pyridyl)ethylene)	n = 4, 10	n = 24	26c
5	$[Cu(mal)_2(picH)_2]\cdot 5H_2O$ (mal = malonate dianion; picH = protonated 2-amino-4-picoline)	n = 4	n = 7	26d
6	$[C_{20}H_{25}SnN_3O_2]\cdot 2.5H_2O$	n = 6	n = 11	26e
7	$[APDO]\cdot 4H_2O$ (APDO = *trans*-4,4′-azopyridine dioxide)	n = 5	n = 8	26f
8	$[(enH_2)_3\{Ni(AEDP)_2\}]\cdot 6H_2O$ (AEDPH_4 = 1-aminoethylenediphosphonic acid; en = ethylenediamine)	n = 6	n = 12	26g
9[a]	$[Cd_2(bpa)_2Cl_4]\cdot 6H_2O$ [bpa = *N*,*N*′-bis(picolinamide)azine]	n = 4	n = 7	26h
10[a]	$[Fe(bipy)_2(CN)_2]\cdot 2.5H_2O$	n = 6	n = 11	26i
11[b]	$[Cu(2\text{-mi})_2(male)]\cdot 3H_2O$ (2-mi = 2-methylimidazole; male = maleate)	n = 4	n = 7	26j

[a] Water molecules are disordered. [b] Hydrogen atoms of the water molecules were not assigned.

and related sytems.[26] For calculations of the one-dimensional water clusters formed by the connectivity between smaller cyclic water clusters, we first calculated the stabilization energy of the small water cluster (fragment) and then the total stabilization energy due to connectivity between the small water cluster units. We have performed all of the calculations at the B3LYP level with a basis set of 6-31+G(d,P),[27] using the *Gaussian 03* software package.[28] For **1**, on basis of the crystal structure geometry, we have made an evaluation of the stability of the water tetramers [O(100) × 2 and O(300) × 2] using the single-point energy calculation without any symmetry constraints. The stabilization energy was found to be −14.57 kcal/mol for the tetramer. Similarly, for the dimer [O(200) and O(400)], it was −2.89 kcal/mol. In the next set of calculations, we have considered the $(H_2O)_{12}$ unit (dodecameric unit) formed by the connectivity between the two tetrameric units and the two dimeric units, which is the basic repeating unit (the total number of hydrogen bonds in this unit is 10) of the water ladder (Figure 3a). The calculated stabilization energy for the $(H_2O)_{12}$ unit was found to be −47.82 kcal/mol. In Figure 3b, we show the plots of the electron densities and electrostatic potentials for the tetrameric and dodecameric units. As can be seen, there appears to be considerable electronic delocalization in the water cluster units due to the hydrogen-bond interactions.

In Figure 4, we have pictorially represented the various water clusters considered for comparison with the water ladders observed in the present compound. One-dimensional water clusters, formed by the connectivity between a tetramer and a monomer, have been observed in the organic host system, $[TACD]\cdot 3H_2O$ (TACD = 1,4,7,10-tetraazacyclododecane; Figure 4a).[26a] Our theoretical evaluation gave an energy of −15.26 kcal/mol for the water tetramer and an overall stabilization energy of −49.36 kcal/mol for the $(H_2O)_{10}$ unit.

One-dimensional water tapes formed by the connectivity between a hexamer and a monomer have been observed in the channels of a metal phosphonocarboxylate network, $[Cd(phen)(Hpppn)]\cdot 4H_2O$ (phen = 1,10-phenanthroline and pppn = 3-phosphonopropionate; Figure 4b).[26b] Here, the calculations reveal a stabilization energy of −26.06 kcal/mol for the hexamer and an overall stabilization energy of −140.81 kcal/mol for the $(H_2O)_{14}$ unit.

Water chains with tetrameric and decameric clusters have been observed in $[Cu^{I}_2Cu^{II}(pydc)_2(bpe)_2]\cdot 7H_2O$ [pydc = pyridine-2,6-dicarboxylate and bpe = *trans*-1,2-bis(4-pyridyl)ethylene; Figure 4c].[26c] Our calculations

(25) (a) Cheruzel, L. E.; Pometun, M. S.; Cecil, M. R.; Mashuta, M. S.; Wittebort, R. J.; Buchanan, R. M. *Angew. Chem., Int. Ed.* **2003**, *42*, 5452. (b) Rather, B.; Zaworotko, M. J. *Chem. Commun.* **2003**, 830. (c) Wakahara, A.; Ishida, T. *Chem. Lett.* **2004**, *33*, 354. (d) Neogi, S.; Bharadwaj, P. K. *Inorg. Chem.* **2005**, 816. (e) Kim, H. J.; Jo, H. J.; Kim, J.; Kim, S. Y.; Kim, D.; Kim, K. *CrystEngComm* **2005**, *7*, 417. (f) Fei, Z. F.; Zhao, D. B.; Geldbach, T. J.; Scopelliti, R.; Dyson, P. J.; Antonijevic, S.; Bodenhausen, G. *Angew. Chem., Int. Ed.* **2005**, *44*, 4720. (g) Zhang, X. L.; Ye, B. H.; Chen, X. M. *Cryst. Growth Des.* **2005**, *5*, 1609. (h) Birkedal, H.; Schwarzenbach, D.; Pattison, P. *Angew. Chem., Int. Ed.* **2002**, *41*, 754. (i) Sreenivasulu, B.; Vittal, J. J. *Angew. Chem., Int. Ed.* **2004**, *43*, 5769. (j) Saha, B. K.; Nangia, A. *Chem. Commun.* **2005**, 3024. (k) Lau, B. Y.; Jiang, F. L.; Yuan, D. Q.; Wu, B. L.; Hong, M. C. *Eur. J. Inorg. Chem.* **2005**, 3214.

(26) (a) Pal, S.; Sankaran, N. B.; Samanta, A. *Angew. Chem., Int. Ed.* **2003**, *42*, 1741. (b) Zhang, X. M.; Fang, R. Q.; Wu, H. S. *Cryst. Growth Des.* **2005**, *5*, 1335. (c) Hu, N. H.; Li, Z. G.; Xu, J. W.; Jia, H. Q.; Niu, J. J. *Cryst. Growth Des.* **2007**, *7*, 15. (d) Choudhury, S. R.; Jana, A. D.; Colacio, E.; Lee, H. M.; Mostafa, G.; Mukhopadhyay, S. *Cryst. Growth Des.* **2007**, *7*, 212. (e) Rolando, L. G.; Berenice, M. D. M.; Victor, B.; Herbert, H.; Hiram, I. B.; Luis, S. Z. R. *Chem. Commun.* **2005**, *44*, 5527. (f) Ma, B. Q.; Sun, H. L.; Gao, S. *Chem. Commun.* **2004**, 2220. (g) Li, M.; Chen, S.; Xiang, J.; He, H.; Yuan, L.; Sun, J. *Cryst. Growth Des.* **2006**, *6*, 1250. (h) Ye, B. H.; Sun, A. P.; Wu, T. F.; Weng, Y. Q.; Chen, X. M. *Eur. J. Inorg. Chem.* **2005**, 1230. (i) Ma, B. Q.; Sun, H. L.; Gao, S. *Eur. J. Inorg. Chem.* **2005**, 3902. (j) Jin, Y.; Che, Y.; Batten, S. R.; Chen, P.; Zheng, J. *Eur. J. Inorg. Chem.* **2007**, 1925.

(27) Becke, A. D. *J. Chem. Phys.* **1993**, *98*, 5648.

(28) Frisch, M. J.; Trucks, G. W.; Schlegel, H. B.; Scuseria, G. E.; Robb, M. A.; Cheeseman, J. R.; Montgomery, J. A.; Vreven, T., Jr.; Kudin, K. N.; Burant, J. C.; Millam, J. M.; Iyengar, S. S.; Tomasi, J.; Barone, V.; Mennucci, B.; Cossi, M.; Scalmani, G.; Rega, N.; Petersson, G. A.; Nakatsuji, H.; Hada, M.; Ehara, M.; Toyota, K.; Fukuda, R.; Hasegawa, J.; Ishida, M.; Nakajima, T.; Honda, Y.; Kitao, O.; Nakai, H.; Klene, M.; Li, X.; Knox, J. E.; Hratchian, H. P.; Cross, J. B.; Adamo, C.; Jaramillo, J.; Gomperts, R.; Stratmann, R. E.; Yazyev, O.; Austin, A. J.; Cammi, R.; Pomelli, C.; Ochterski, J. W.; Ayala, P. Y.; Morokuma, K.; Voth, G. A.; Salvador, P.; Dannenberg, J. J.; Zakrzewski, V. G.; Dapprich, S.; Daniels, A. D.; Strain, M. C.; Farkas, O.; Malick, D. K.; Rabuck, A. D.; Raghavachari, K.; Foresman, J. B.; Ortiz, J. V.; Cui, Q.; Baboul, A. G.; Clifford, S.; Cioslowski, J.; Stefanov, B. B.; Liu, G.; Liashenko, A.; Piskorz, P.; Komaromi, I.; Martin, R. L.; Fox, D. J.; Keith, T.; Al-Laham, M. A.; Peng, C. Y.; Nanayakkara, A.; Challacombe, M.; Gill, P. M. W.; Johnson, B.; Chen, W.; Wong, M. W.; Gonzalez, C.; Pople, J. A. *Gaussian 03*, revision B.05; Gaussian, Inc.: Pittsburgh, PA, 2003.

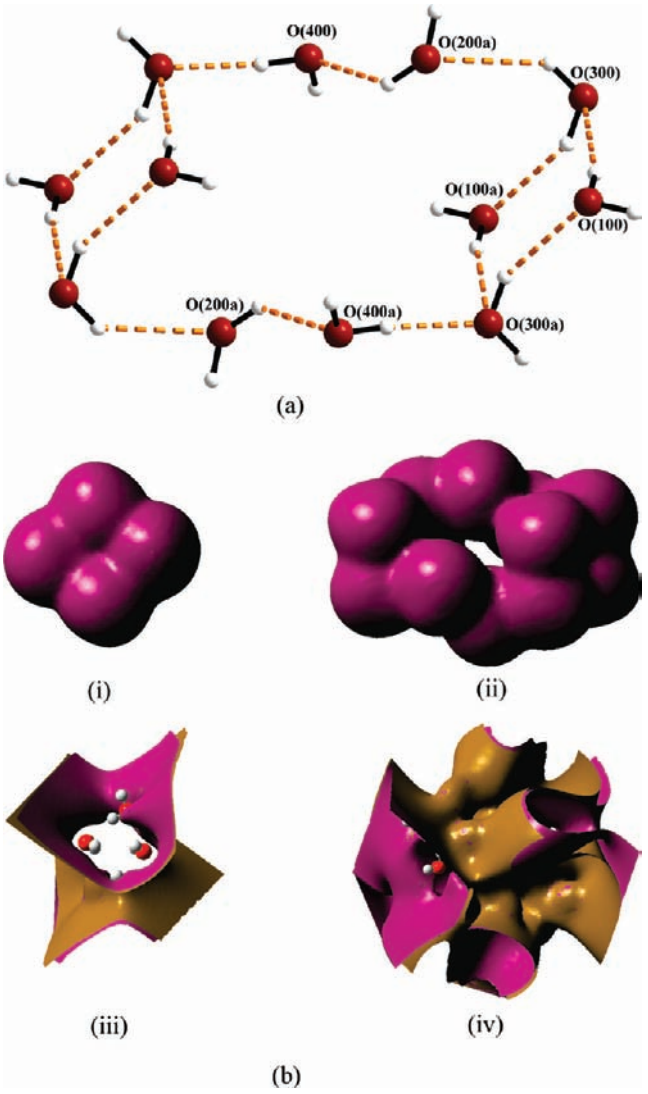

Figure 3. (a) One decameric water cluster unit present in the one-dimensional water ladders in **1**, which was used for the calculation of the stabilization energy (see the text). (b) Plots of the electron densities: (i) the tetramer [O(100) × 2 + O(300) × 2], (ii) the dodecamer, $(H_2O)_{12}$. Plots of the electrostatic potentials: (iii) the tetramer, (iv) the dodecamer.

yielded a stabilization energy of −80.57 kcal/mol for the decameric cluster and −31.6 kcal/mol for the tetramer. The overall stabilization energy of −199.09 kcal/mol has been obtained for the $(H_2O)_{24}$ unit.

In all of these cases, the cyclic water clusters are connected by smaller linkers such as a monomer, a dimer, or a tetramer of water, giving rise to one-dimensional water chains. This is similar to the water ladder observed in the present compound. In the literature, there are reports of other one-dimensional water clusters formed by sharing through the corners or edges, and we have performed a similar study on these water molecules as well.

The formation of one-dimensional water chains by corner sharing of tetrameric units has been observed in $[Cu(mal)_2(picH)_2]\cdot 5H_2O$ (mal = malonate dianion and picH = protonated 2-amino-4-picoline; Figure 4d).[26d] The stabilization energy of −28.32 kcal/mol has been obtained for the tetramer, and the overall stabilization energy of −55.43 kcal/mol has been obtained for the connected tetramers, $(H_2O)_7$. Comparable values have been reported for this cluster.[26d]

Another example of this type of water cluster is the formation of one-dimensional chains by sharing between the cyclic hexamer units in $[C_{20}H_{25}SnN_3O_2]\cdot 2.5H_2O$ (Figure 4e).[26e] Here, the stabilization energy was found to be −20.46 kcal/mol for the hexamer, and the total stabilization energy for the two-connected hexamer, $(H_2O)_{11}$, was found to be −46.49 kcal/mol.

One-dimensional water clusters have also been observed by the edge sharing of cyclic water pentamer units in the organic host, $[APDO]\cdot 4H_2O$ (APDO = *trans*-4, 4′-azopyridine dioxide; Figure 4f).[26f] We obtained a stabilization energy of −13.44 kcal/mol for the water pentamer and a total stabilization energy of −27.66 kcal/mol for the two-connected pentamer, $(H_2O)_8$ unit.

One-dimensional water clusters have also been observed in the proton-transfer salt host, $(enH_2)_3[Ni(AEDP)_2]\cdot 6H_2O$ (AEDPH4 = 1-aminoethylenediphosphonic acid and en = ethylenediamine; Figure 4g).[26g] Here, the calculations show a stabilization energy of −36.97 kcal/mol for the hexamer and −81.41 kcal/mol for the two-connected hexameric unit, $(H_2O)_{12}$.

The calculations on the various one-dimensional water structures gave an opportunity to correlate the stabilization energies with the number of water molecules (n) of various $(H_2O)_n$ units observed in different host−guest systems. The stabilization energies are plotted against n (see the Supporting Information, Figure S11). As can be noted, the stabilization energies are not linear with the size of the $(H_2O)_n$ units (n = 2−12). Additionally, $(H_2O)_n$ clusters with similar n values appear to have different energies. This behavior suggests that the stabilization energies of the water clusters depend not only on n but also on other factors such as distances and angles between the water molecules and the size and shape of the water cluster units.

Dynamics of the Water Molecules. Thermogravimetric analysis (TGA) was performed to investigate the thermal stability of the water structure as well as the framework of **1** (see the Supporting Information, Figure S12). TGA was carried out (Mettler-Toledo) in an oxygen atmosphere (flow rate = 20 mL/min) in the temperature range of 30−850 °C (heating rate = 5 °C/min). The TGA studies show an initial weight loss of 17% in the temperature range of 50−180 °C, which is consistent with the calculated value of 17.3% for the loss of the extraframework and coordinated water molecules. The second sharp weight loss at ∼ 400 °C corresponds with the loss of the carboxylate units. The total observed weight loss of 68% corresponds well with the loss of the carboxylate and water molecules (calcd 66.7%). The final calcined product was found to be crystalline by PXRD and corresponds with a mixture of Gd_2O_3 (JCPDS: 12-0797) and NiO (JCPDS: 47-1049).

Because the initial weight loss was observed below 200 °C and also corresponded with the loss of water molecules, we wanted to examine the possible reversible nature of the water adsorption in the sample. For this, the sample was taken in the TGA apparatus (Figure 5a) and heated from 30 to 180 °C (heating rate = 5 °C/min), keeping the sample for 30 min at 180 °C. This was followed by cooling

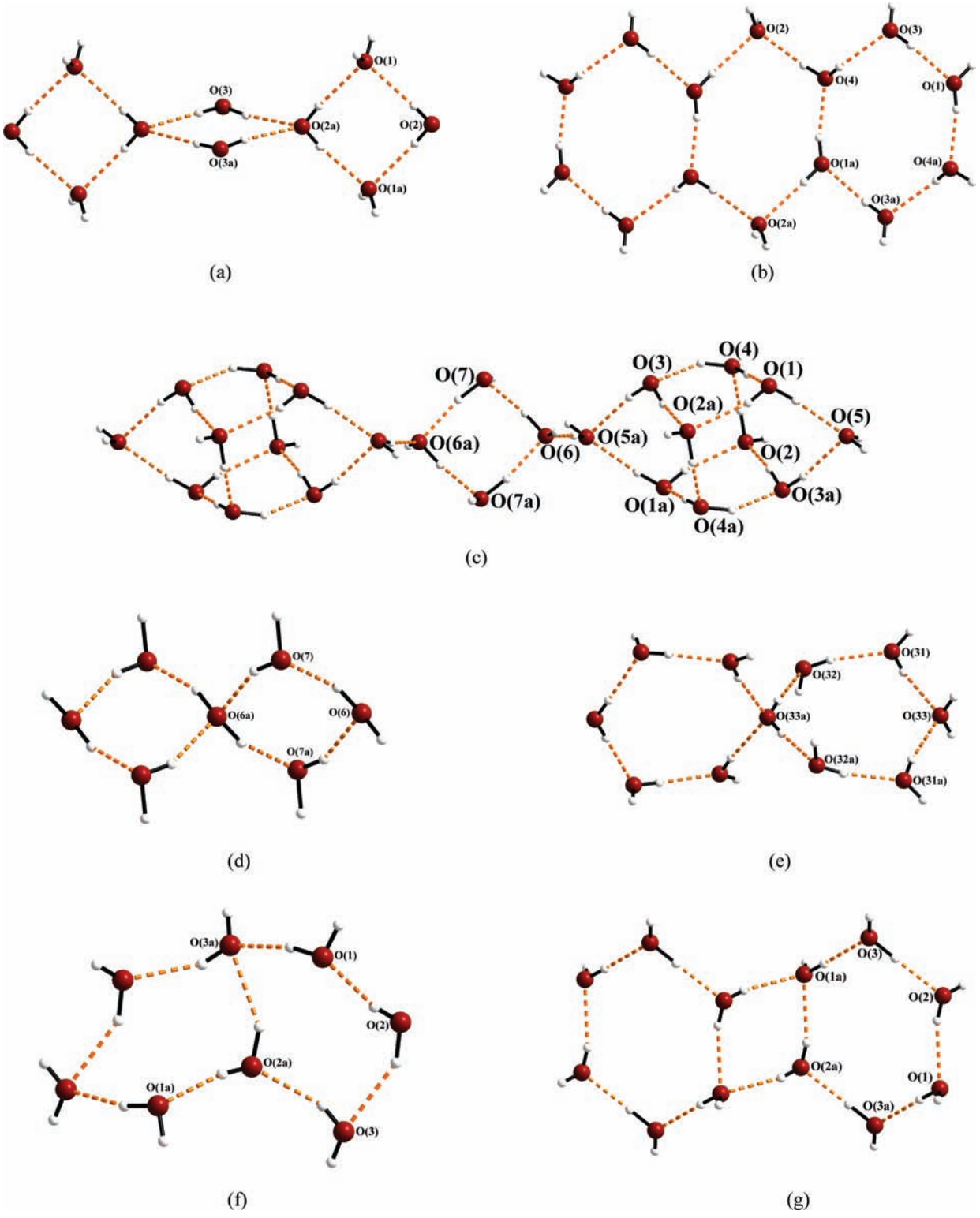

Figure 4. Various one-dimensional water structures from the literature and compared in the present study (only the fragment of the water cluster used in the calculations is shown): (a) water decamer unit in [TACD]·3H_2O (TACD = 1,4,7,10-tetraazacyclododecane);[26a] (b) water $(H_2O)_{14}$ unit in [Cd(phen)(Hpppn)]·4H_2O (phen = 1,10-phenanthroline; pppn = 3-phosphonopropionate);[26b] (c) water $(H_2O)_{24}$ unit in $[Cu^{I}_2Cu^{II}(pydc)_2(bpe)_2]\cdot 7H_2O$ [pydc = pyridine-2,6-dicarboxylate; bpe = *trans*-1,2-bis(4-pyridyl)ethylene];[26c] (d) water heptamer in $[Cu(mal)_2(picH)_2]\cdot 5H_2O$ (mal = malonate dianion; picH = protonated 2-amino-4-picoline);[26d] (e) water $(H_2O)_{11}$ unit in $[C_{20}H_{25}SnN_3O_2]$b2.5H_2O;[26e] (f) water octamer in [APDO]·4H_2O (APDO = *trans*-4,4′-azopyridine dioxide);[26f] (g) water $(H_2O)_{12}$ unit in $[(enH_2)_3\{Ni(AEDP)_2\}]\cdot 6H_2O$ (AEDPH_4 = 1-aminoethylenediphosphonic acid; en = ethylenediamine).[26g]

to 30 °C (cooling rate = 2 °C/min) along with the introduction of water vapor (75 min) and also cooling for 1 h at 30 °C. In this rehydation process, the dry sample returns to 98.9% of the initial weight of the original sample from 83% at the completely dehydrated state. The dehydration and rehydration processes were repeated four times, and in each case, similar behavior was observed. The final sample after the four cycles of

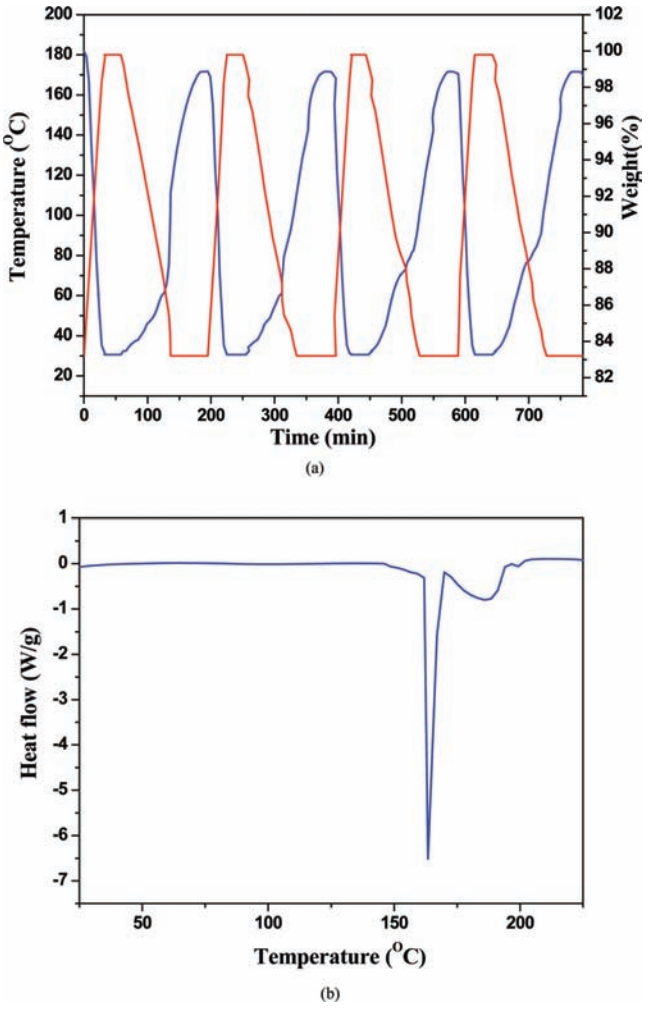

Figure 5. (a) Reversible water uptake study of **1** using TGA. The red curve represents the heating and cooling cycle. The blue trace shows the weight loss and weight gain. (b) Differential scanning calorimetry (DSC) study of **1**. Note the three endothermic peaks.

dehydration−rehydration was examined by PXRD, which indicated the same PXRD pattern as the original sample (see the Supporting Information, Figure S14). This indicates that the water molecules are fully reversible. Our efforts to investigate the dehydrated phase (in situ) using the single-crystal XRD were not successful because the sample appears to lose the single crystalline nature upon removal of the water molecules.

The dehydration/removal of the water molecules also brings about a change in the color of the sample. Thus, the compound changes from light greenish blue to brown after dehydration. The dehydrated sample, brownish in color, returns to the original color within 5 min upon exposure to atmospheric conditions (see the Supporting Information, Figure S15). This change of color could be due to the change of the crystal-field-splitting energy of the Ni^{2+} ions, where the Ni^{2+} ions change from the octahedral state to the four-coordinated state, possibly a highly distorted tetrahedral coordination, after removal of the bound water molecules.[29]

(29) Gill, N. S.; Taylor, F. B.; Hatfield, W. E.; Parker, W. E.; Fountain, C. S.; Bunger, F. L. Tetrahalo complexes of Dipositive Metals in the First Transition Series. *Inorganic Syntheses*; Tyree, S. Y., Jr., Ed.; McGraw-Hill, Inc.: New York, 1967; Vol. 9, pp 136−142.

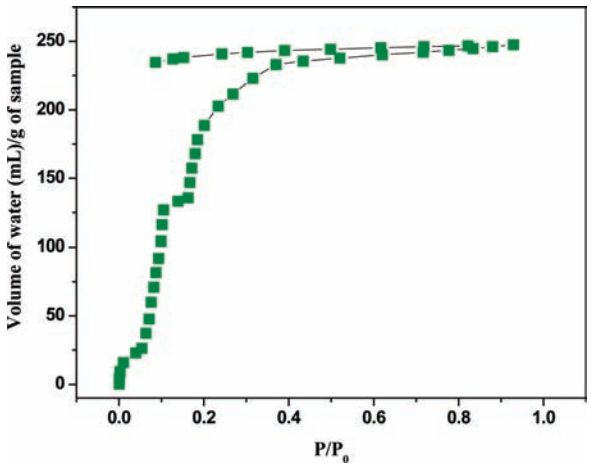

Figure 6. Water vapor adsorption−desorption isotherms of **1**.

We have also carried out DSC measurements in the temperature range of 25−225 °C (heating rate = 5 °C/min) to learn about the energetics of the dehydration process (Figure 5b). The DSC studies indicate that the dehydration process is endothermic with three distinct peaks at 163, 186, and 200 °C, respectively. The three peaks probably correspond with removal of the water molecules from different environments in the crystal structures. The total molar enthalpy calculated from the DSC measurements is 55.46 kcal, which corresponds with an energy of 4.62 kcal per water molecule. Similar values have been obtained previously.[25a]

Encouraged by the stability of the framework and the reversibility of the hydration−dehydration cycles, we sought to investigate the sorption behavior. For this, a preheated sample (~180 °C) was used and the adsorption studies were carried out using nitrogen and water as the probe molecules. The adsorption isotherms of N_2 at 77 K indicate no significant uptake of nitrogen, and only surface adsorption was observed (see the Supporting Information, Figure S16). Water adsorption, measured at 298 K, shows a gradual uptake, and a total of 248 mL/g (11.42 mol of H_2O/mol of **I**) was adsorbed at $P/P_0 = 1$ (Figure 6). The observed rapid onset of water vapor sorption at very low pressures is characteristic of the presence of micropores in the solid. Figure 6 also shows considerable hysteresis in the desorption curve, which indicates that the dry sample has a high affinity for the water molecules. Similar behavior has been reported by Kitagawa et al. for $[Gd_2(imidc)_2(H_2O)_3](H_2O)$,[30] which shows reasonable water vapor sorption but nonporous behavior toward N_2 in its dehydrated state.

Optical, Magnetic, and Electron Paramagnetic Resonance (EPR) Studies. The diffuse-reflectance UV−vis spectra at room temperature were recorded for the sodium salts of 1,2-bdc and 2,5-pydc and for the present compound (see the Supporting Information, Figure S17). In all cases, the main absorption bands are at ~280 nm, which may be due to the intraligand absorption (ILA; $n \rightarrow \pi^*$ or $\pi \rightarrow \pi^*$). The low intense peak at ~400 nm for the sodium salt of 2,5-pydc may be due to the ILA of the heterocyclic aromatic system, which was not observed in

(30) Maji, T. K.; Mostafa, G.; Chang, H. C.; Kitagawa, S. *Chem. Commun.* **2005**, 2436.

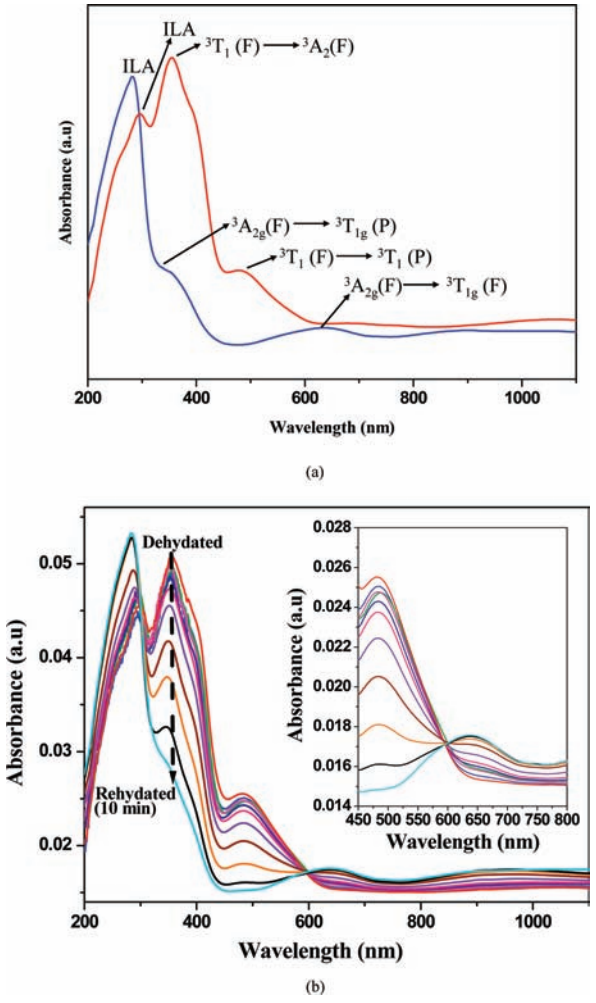

Figure 7. (a) UV−vis spectra of **1** (blue trace) and the dehydrated phase (red trace). (b) UV−vis spectra of the dehydrated sample after exposure to the atmosphere for various times (0−10 min). The inset shows the spectra in the range of 450−800 nm.

the present compound because of the presence of Ni^{2+} ions. A shoulder at 330 nm and a broad band at ~635 nm were also observed for **I**, which may be due to the d−d transition of the $d^8(Ni^{2+})$ ion. These absorptions at 330 and 635 nm can be assigned to the $^3A_{2g}(F) \rightarrow {}^3T_{1g}(P)$ and $^3A_{2g}(F) \rightarrow {}^3T_{1g}(F)$ transitions, respectively.[31] The electronic transitions from the Gd^{3+} ions ($4f^7$) could not be observed clearly because the excited-state energy for the Gd^{3+} ion is high, with the lowest-energy transition ($^8S \rightarrow {}^6P_{7/2}$) generally appearing at $\lambda < 300$ nm, which overlaps with the strong intraligand bands observed for **1**.[32]

The change of color from greenish blue to brown upon dehydration suggested the possibility of studying the changes in the electronic transitions in the dehydrated sample. For this, the compound was heated under vacuum in a glass tube for 2 h at 180 °C and the resulting brown sample was carefully transferred to a quartz-sealed cuvette under inert conditions (glovebox). The UV−vis spectra of the dehydrated sample was recorded at room temperature (Figure 7a). As can be noted, the UV−vis spectrum of the dehydrated compound show differences from that of the original compound. The ILA band of the dehydrated phase shows a 10 nm shift and appears at 290 nm. The absorption bands at 355 and 485 nm probably originate from the d−d transition of the four-coordinated $d^8(Ni^{2+})$ ions. The absorption bands can be assigned to the $^3T_1(F) \rightarrow {}^3A_2(F)$ and $^3T_1(F) \rightarrow {}^3T_1(P)$ transitions, respectively, based on a distorted tetrahedral geometry of Ni^{2+} ions.[31] Thus, the light greenish blue of the hydrated compound and the brown of the dehydrated sample could be due to the $^3A_{2g}(F) \rightarrow {}^3T_{1g}(F)$ and $^3T_1(F) \rightarrow {}^3T_1(P)$ transitions in the visible region. The relative intensity of the observed d−d transition for the octahedral Ni^{2+} ions appears to be low because this transition is Laporte-forbidden. The light greenish blue of the original compound is due to vibronic coupling of the octahedral Ni^{2+} ions, while a comparatively intense d−d transition (darker brown) of the dehydrated sample may be due to partially Laporte-allowed transitions (d−p mixing) of the tetrahedral Ni^{2+} ions.[33]

To investigate of the rehydration behavior more clearly, the UV−vis spectra of the dehydrated samples were studied by exposing the sample to atmospheric conditions (Figure 7b). As can be noted, the intensities of the $^3T_1(F) \rightarrow {}^3A_2(F)$ and $^3T_1(F) \rightarrow {}^3T_1(P)$ transitions decrease continuously along with an increase in the intensity of the $^3A_{2g}(F) \rightarrow {}^3T_{1g}(F)$ transition as a function of time. This observation corresponds well with the change of color from brown to greenish blue.

Room-temperature solid-state photoluminescence (PL) studies were carried out on ground samples (see the Supporting Information, Figure S18). The aromatic dicarboxylates used in the formation of MOFs absorb strongly in the UV region and are an attractive ligands for sensitizing the lanthanide ion (Eu, Dy, Sm, and Tb) via the antenna effect.[34] On the other hand, MOF compounds of Gd do not show this behavior because of the absence of any ionic resonance levels below the triplet state of the ligand.[35] The emission spectra of the sodium salts of 1,2-bdc and 2,5-pydc and **1** exhibit a main emission band at ~425 nm, which can be assigned to the intraligand luminescence ($\pi^* \rightarrow$ n or $\pi^* \rightarrow \pi$). The additional peak for the sodium salt of 2,5-pydc and **1** at ~485 nm may be due to the intraligand transition arising from the heterocyclic system (pyridine).

Temperature-dependent magnetic susceptibility measurement for **1** has been performed on well-ground samples using a SQUID magnetometer in the 2−300 K temperature range, with an applied field of 1000 Oe (see the Supporting Information, Figure S19). The observed effective magnetic moment of the present compound at room temperature (300 K) is 18.12 μ_B, which is very close to the value expected for two Gd^{3+} ions and one Ni^{2+} ion ($\mu_{spin\text{-}only}$ for Gd^{3+} is 7.93 and for Ni^{2+} is 2.83).

(31) Lever, A. B. P. *Inorganic Electronic Spectroscopy*; Elsevier: New York, 1968.
(32) Blasse, G.; Grabmaier, B. C. *Luminescent Materials*; Springer-Verlag: Heidelberg, Germany, 1994.
(33) Huhhey, J. .E; Keiter, E. A.; Keiter, R. L. *Inorganic Chemistry: Principles of structure and reactivity*, 4th ed.; Pearson Education: Upper Saddle River, NJ, 2000.
(34) (a) Serre, C.; Pelle., F.; Gardant, N.; Ferey, G. *Chem. Mater.* **2004**, *16*, 1177. (b) Millange, F.; Serre, C.; Marrot, J.; Gardant, N.; Pelle, F.; Ferey, G. *J. Mater. Chem.* **2004**, *14*, 642. (c) Serre, C.; Millange, C.; Thouvenot, N.; Gardant, N.; Pelle, F.; Ferey, G. *J. Mater. Chem.* **2004**, *14*, 1530.
(35) Chandler, B. D.; Cramb, D. T.; Shimizu, G. K. H. *J. Am. Chem. Soc.* **2006**, *128*, 10403.

The Gd^{3+} ions do not have any orbital contribution because L (orbital quantum number) for f^7 system is 0, and for the case of Ni^{2+}, the orbital contributions are completely suppressed for the octahedral geometry with a $t_{2g}^6 e_g^2$ electronic configuration in the ground state. The $1/\chi_M$ vs T curve is shown as an inset of Figure 12. Above 100 K, the magnetic behavior can be fitted to the Curie–Weiss law, with $C = 10.41$ emu/mol and $\theta_p = -3.18$ K. The small negative value of θ_P indicates weak antiferromagnetic interactions.

The EPR spectrum at room temperature was recorded with diphenylpicrylhydrazyl as the standard (see the Supporting Information, Figure S20). Two bands observed with a superposition at $g = 2.34$ and 1.83 corresponds with the Gd^{3+} ions.[36] EPR spectra corresponding to Ni^{2+} have not been observed because of the weak EPR signal of the Ni^{2+} ions.

Conclusions

One-dimensional water ladders, occupying the interlamellar spaces, appear to be reversibly adsorbed along with changes in the color of the sample. The fast response of the dehydrated sample to the presence of water suggests that this compound could be employed as a water sensor. Stabilization energies of the water molecules, calculated using density functional theory, suggest that the values are comparable to other similarly reported water structures. The role of hydrated transition-metal ions in MOFs is still not explored fully, and the present study suggests that other related compounds could be prepared with as yet unexplored properties. Research in this direction is presently underway.

Acknowledgment. S.N. thanks the Department of Science and Technology, Government of India, for the award of a research grant, and the authors thank the Council of Scientific and Industrial Research, Government of India, for the award of a fellowship (to P.M.) and a research grant. S.N. also thanks the Department of Science and Technology, Government of India, for the award of the RAMANNA fellowship.

Supporting Information Available: X-ray crystallographic files in CIF format, bond angle table, hydrogen-bond table, additional structural plots, IR, TGA, PXRD, stabilization energy plot of water clusters, image of samples in hydrated and dehydrated states, and N_2 adsorption, UV, PL, magnetic, and EPR plots. This material is available free of charge via the Internet at http://pubs.acs.org.

(36) Szyczewski, A.; Lis, S.; Kruczynski, Z.; But, S.; Elbanowski, M.; Pietrzak, J. *J. Alloys Compd.* **1998**, *275–277*, 349.